

Hodgkin-Huxley Type Model of the Auditory Nerve

Joshua Goldwyn

March 15, 2006

1 Introduction

The foundation for most mathematical models of neural dynamics is the Hodgkin-Huxley model. This canonical model has four variables: Voltage potential across the cell membrane of a neuron and three variables that represent permeability of ion channels in the cell membrane. This model was developed by Hodgkin and Huxley in their research on the squid's giant axon in the 1950's. It successfully captures many of the characteristic dynamics of neurons including the threshold behavior that allows neurons to generate action potentials (or "spikes" of current) in response to a small perturbation from their rest potential, as well as more subtle dynamics such as oscillatory behavior under the right conditions (Murray, 2002).

Hodgkin and Huxley developed their model based on their research on the squid's giant axon. However, there are many other types of nerve cells with their own unique physiological features and their own characteristic behaviors. The Hodgkin-Huxley model can provide the basic framework for modeling a variety of neural dynamics, but modifications must be made for further insight into particular neurons.

In this paper, we review a Hodgkin-Huxley type model of the auditory nerve (AN) and explore particular behaviors of the auditory nerve that we can investigate using this mathematical model. We will also discuss more recent research that argues for including stochastic elements into the deterministic Hodgkin-Huxley model.

2 The Auditory Nerve

2.1 Physiology of the AN

In the mammalian inner ear, sound waves propagate through the ear and into a structure in the inner ear called the cochlea. The cochlea is a fluid filled chamber containing three membranes. The effect of an incoming sound wave is to generate traveling waves

in the cochlear fluid as well as along the basilar membrane. The basilar membrane is lined with hair cells. The traveling waves and membrane oscillations in the cochlea generate vibrations of the hair cells. The movement of the hair cells, which are innervated by the auditory nerve, induces a change in the electrical charge of these cells. This change in charge generates a response in the auditory nerve, and thus acoustic waves are transduced into electrical pulses that are received by the auditory nerve (Geisler, 1991).

The AN itself is a collection of axons numbering in the tens of thousands in mammals. There are two types of auditory nerves. Little is known about Type 2 neurons, but Type 1 are large with long myelinated axons and fast responses (Borisyuk, 2005). The length and size of these cells is distinct enough from the squid's giant axon to warrant mathematical models particular for these neurons (Colombo and Parkins, 1987).

2.2 Cochlear Implants

Modeling the response of the AN to electrical stimuli has important medical benefits. Many patients with hearing disorders are treated with a device called a cochlear implant. This device directly stimulates the AN of a patient with electrical currents, simulating the action of hair cells. The effectiveness and design of cochlear implants, therefore, depends on our knowledge of the response of the AN to electrical pulses.

3 Mathematical Modeling of the AN

3.1 Colombo-Parkins Model

Colombo and Parkins developed a deterministic, Hodgkin-Huxley type model in the late 1980's using modifications and parameter values specific for the physiology of the AN (Colombo and Parkins, 1987). Their model (hereafter referred to as the CP model) consists of two components: a Frankenhauser-Huxley (FH) Model (to be analyzed in Section

4) combined with a McNeal Model. They model a collection of 8 axons and the McNeal Model describes the dependence of voltage potential change across the membrane of one neuron on the membrane potential of adjacent neurons. The governing equations for the McNeal Model are:

$$\begin{aligned}\frac{dV_n}{dt} &= \frac{1}{C_m} [g_a(V_{n-1} - 2V_n + V_{n+1} + V_{e,n-1} - 2V_{e,n} + V_{e,n+1} - g_m V_n)] \text{ for } n \neq 0 \\ \frac{dV_0}{dt} &= \frac{1}{C_m} [g_a(V_{-1} - 2V_0 + V_1 + V_{e,-1} - 2V_{e,0} + V_{e,1} - pdl(I_{Na} + I_K + I_L + I_P))] \text{ for } n = 0.\end{aligned}$$

(see Colombo and Parkins (1987) for definition and values of parameters).

This is a coupled, linear system with one equation for each neuron included in the model. In the analysis that follows, only one neuron will be modeled so these equations will be neglected and a single equation for $\frac{dV}{dt}$ will be used. But it is important to note that, given that the AN is a collection of tens of thousands of neurons, a model that takes into account the influence of neighboring neurons should provide much more realistic results. Furthermore, the way in which the CP model is specifically tailored to model the AN is in the parameter values in these McNeal equations because the size and spacing of nerve fibers affects how neighboring neurons interact with one another. The parameter values used by Colombo and Parkins are based on known physiological specifications of the mammalian AN.

Our analysis will focus on the FH Model used by Colombo and Parkins. Colombo and Parkins use the above McNeal equations to model voltage across the cell membrane and model the permeability of the cell membranes to various ions based on the work of Frankenhauser and Huxley. The FH model is a modified version of the well known Hodgkin-Huxley model. The FH model (Frankenhauser and Huxley, 1963) models myelinated nerve fibers and the main distinction between the FH model and the canonical Hodgkin-Huxley model is the inclusion of the variable p which is related to a “non-specific current” I_p . Frankenhauser and Huxley found similarities between myelinated

nerve fibers and the squid’s giant axon. In particular, they found that most currents are carried by potassium and sodium (including the non-specific current which was found to be mostly potassium) in both nerve types. But there are significant differences, notably the rate constants for permeability changes and differences in rectification properties (how permeability of the membrane responds to changes in ion concentration on either side of the cell membrane).

The governing equations for this deterministic model of a neuron are:

$$\begin{aligned}\frac{dV}{dt} &= \frac{1}{C_m}(I - (I_{Na} + I_K + I_p + I_L)) \\ \frac{dm}{dt} &= \alpha_m(1 - m) - \beta_m m \\ \frac{dh}{dt} &= \alpha_h(1 - h) - \beta_h h \\ \frac{dp}{dt} &= \alpha_p(1 - p) - \beta_p p \\ \frac{dn}{dt} &= \alpha_n(1 - n) - \beta_n n.\end{aligned}$$

(Definitions of parameter values can be found in MATLAB code attached or in the papers of Colombo and Parkins or Frankenhauser and Huxley. It should be noted that α and β are not constant parameters, but rather nonlinear functions of V . Additionally, the ion currents are nonlinear functions of the variables m, n, p and h .)

3.2 Stochastic Improvements

This paper focuses on modeling the auditory nerve response to electrical pulses using a deterministic model. Deterministic models, especially Hodgkin-Huxley type models, are useful because they are well understood mathematically and capture many of the basic features of neurons. However, experimental data reveal that the neural response to electrical stimulation is not purely deterministic. For example, in response to stimuli from cochlear implants, it is now thought that neurons fire based on a probability dis-

tribution with a fairly high variance. In other words, if an electrical pulse is delivered by a cochlear implant to the AN, instead of a guaranteed response in the neuron (as a deterministic model would predict), the neuron may or may not fire. The likelihood that the neuron responds with an action potential can be modeled with a probability distribution. So this process could be more accurately modeled with stochastic methods.

The stochasticity in neural dynamics comes from random fluctuations in membrane potentials. These fluctuations are negatively correlated with the diameter of the nerve fiber. So while squid axon of Hodgkin and Huxley (mean diameter of $500/\mu\text{m}$) may be relatively free of such randomness, it may not be reasonable to neglect this effect in mammalian AN fibers (mean diameter of $2 - 4\mu\text{m}$) (Bruce et al, 1999a, 1999b).

Bruce et al have incorporated stochastic elements into a model of the AN's response to single pulse (1999a) and multiple pulses (1999b), and have been able to fit their simulation results to experimental data much better than would be possible with a deterministic model.

4 Analysis of the Frankenhauser-Huxley Model

The FH Model effectively models several important features of the AN response to electrical stimuli. In the mathematical analysis that follows, two important features are investigated. First, we look at the generation of action potential of “spikes.” Second, we look at the AN response to multiple pulses. In particular, we will analyze a phenomenon known as the “refractory effect.” This refers to the observable fact that for a period of time after a spike, no new spikes can be generated regardless of the electrical stimulus applied to the neuron.

4.1 Stability and Spikes

Basic to any model of neural dynamics is the generation of an action potential in response to an action potential.. The Hodgkin-Huxley model captures this dynamic (Murray, 2002) as does the FH model. Figure 1 displays the results of numerically solving the FH model in MATLAB with the parameter values used by Colombo and Parkins in their AN model (Colombo and Parkins, 1987; Frankenhauser and Huxley, 1963). The data in Figure 1 is the result of applying a 1mA pulse of current during the time $0\text{ms} < t < 0.1\text{ms}$ and leaving the system unperturbed at all other times.

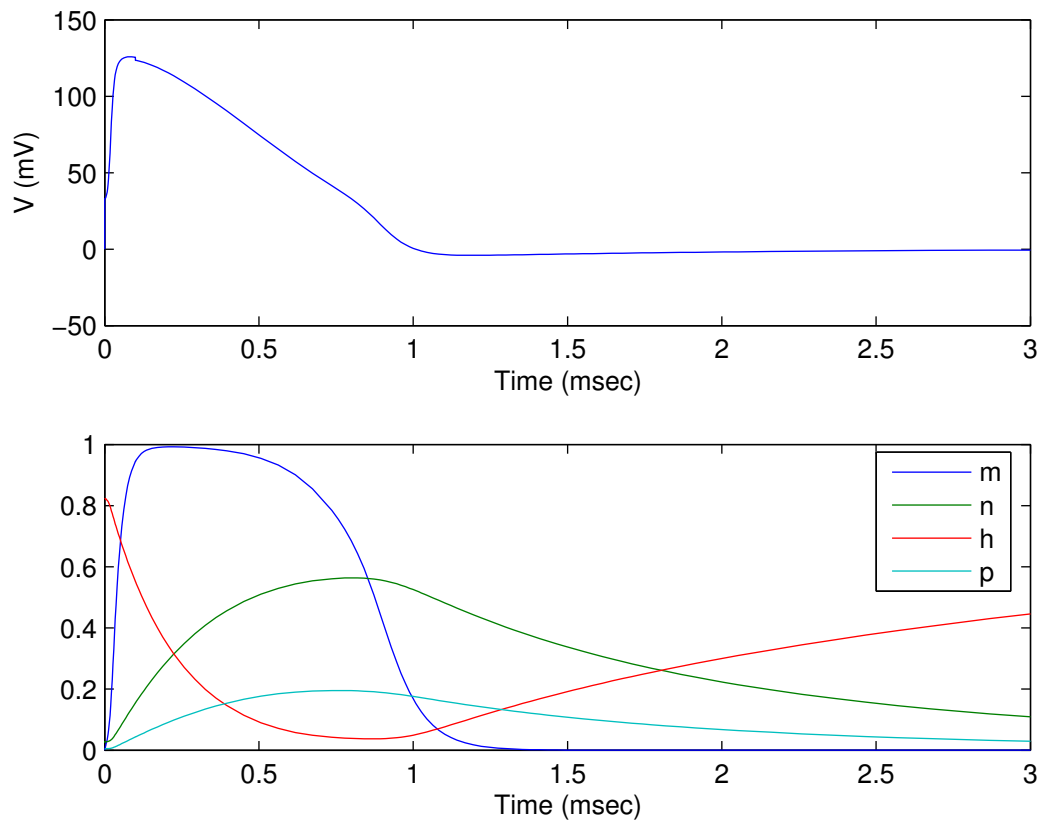


Figure 1: Computed Action Potential, response to 0.1msec pulse of 1mA.

This large spike in voltage away from the steady state in response to a sufficient perturbation in current is known as a threshold phenomenon. In the auditory nerve,

this is the mechanism by which auditory stimuli are transmitted to the brain where sounds are interpreted and processed.

In terms of the mathematical model, a spike can only be generated when an unstable equilibrium state exists. To analyze the stability of the system of equations that make up the FH model, we make several simplifications and reduce the system of equations to two equations (V and m) (Fitzhugh, 1959).

The following analysis follows the work of Borisyuk and Rinzel (2004). The equations for m, n, h and p have the following form:

$$\dot{x} = \alpha_x(V)(1 - x) - \beta_x(V)x.$$

Dividing both sides of the equation by $\alpha_x + \beta_x$, the equation becomes:

$$\tau_x \dot{x} = x_\infty(V) - x.$$

where $\tau_x = \frac{1}{\alpha_x + \beta_x}$ and $x_\infty(V) = \frac{\alpha_x}{\alpha_x + \beta_x}$. Dimensional analysis shows that τ_x has units of time so this can be thought of as the timescale of x . Furthermore, setting the derivative equal to 0 reveals that $x_\infty(V)$ is the equilibrium value of x . Figure 2 plots the timescales of the four variables.

From Figure 2, observe that the timescale of m is an order of magnitude less than the timescales of the other variables. So define this to be a “fast” variable and the others to be “slow” variables. Then, on a short timescale, the slow variables are approximately constant and the fast variable is approximately equal to its equilibrium value, and the equation for voltage can be rewritten as a function of the “instantaneous current”

$$\frac{dV}{dt} = \frac{1}{C_m}(-I_{inst})$$

where I_{inst} is a function of $V, m_\infty, h_0, n_0, p_0$ and x_0 is the initial value of the variable x

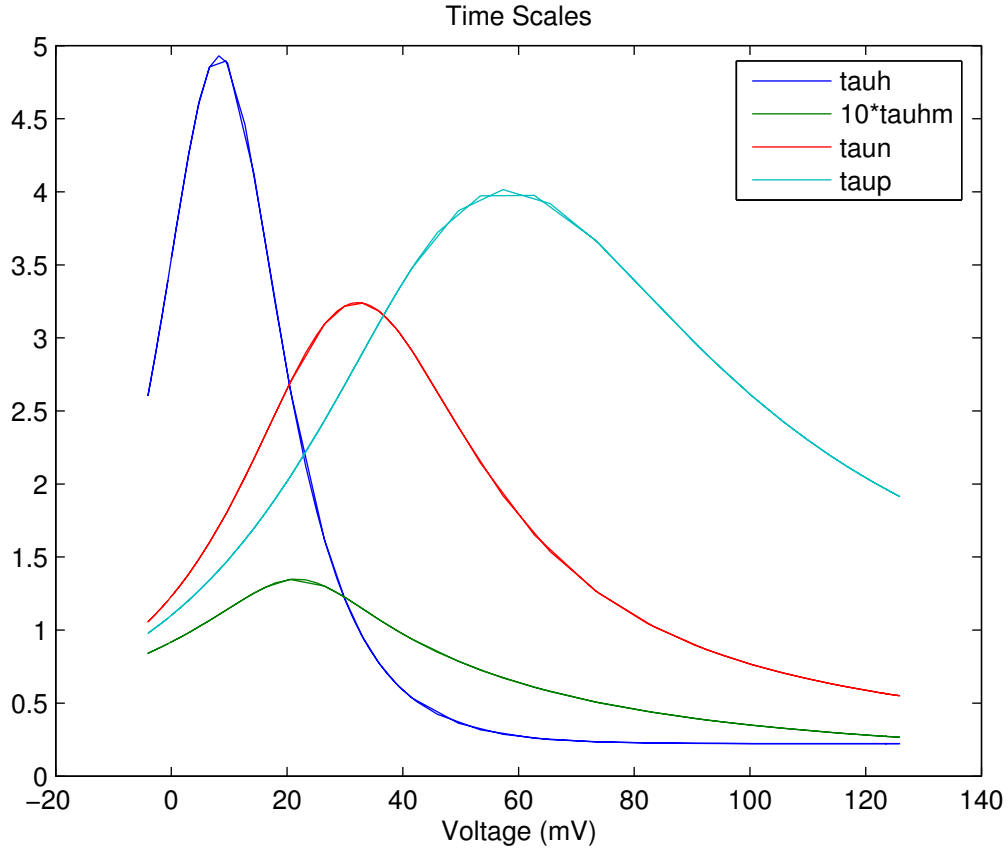


Figure 2: The m timescale is an order of magnitude less than the other variables

in the short time period of interest.

With this simplification, linear stability analysis becomes tractable. Let V^* be an equilibrium voltage in the presence of some applied current I_{app} . Then if V^* is perturbed to $V^* + v$ (for $0 < v \ll 1$), we get the following:

$$\begin{aligned} \frac{d}{dt}(V^* + v) &= \frac{1}{C_m}(-I_{inst}(V^* + v) + I_{app}) \\ \Rightarrow \frac{dv}{dt} &= \frac{1}{C_m}(-I_{inst}(V^*) - \frac{dI_{inst}(V^*)}{dV}v + O(v^2) + I_{app}) \end{aligned}$$

By definition of the equilibrium state, the first and last terms cancel out. So the linear approximation becomes

$$\frac{dv}{dt} = -\frac{1}{C_m} \left(\frac{dI_{inst}(V^*)}{dV} v \right).$$

In other words stability is determined by the slope of $I_{inst}(V)$: positive slope implies stability and negative slope implies an unstable equilibrium. Figure 3 plots I_{inst} as a function of V , beginning from an equilibrium state with no applied current.

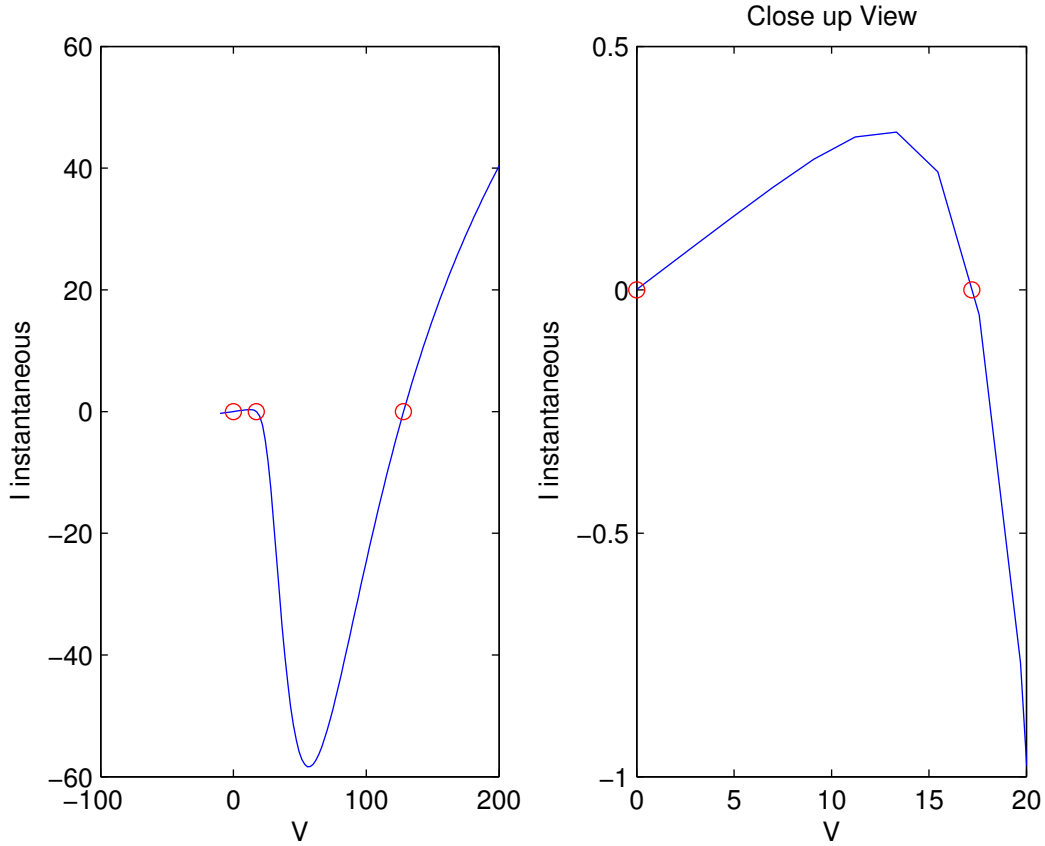


Figure 3: Three Equilibrium Points, middle point is unstable

From Figure 3, observe that in the absence of an applied current, the instantaneous current curve has three roots which correspond to the system of equations having three equilibrium points. Furthermore, the middle equilibrium point is unstable since the slope of $I_{inst}(V)$ is negative there. So if a voltage change of greater than approximately 17mV, is applied to the system, the system will become unstable and move toward the upper equilibrium point at $V \approx 130$ mV. Thus the threshold phenomenon seen in Figure 1 is predicted in terms of equilibria and stability analysis of the unperturbed system, where our analysis has relied on the simplifying assumptions of fast and

slow timescale dynamics of the variables. Biologically speaking, we can conclude that the model accurately captures the phenomenon of the generation of action potentials in a neuron.

4.2 Refractory Effect

Immediately after an action potential is generated there is a period of time during which the neuron cannot spike again regardless of what current or voltage changes are applied to it. This phenomenon is observed in physiological data and is known as the “refractory effect” (Bruce et al, 1999b). The refractory effect can be split into two periods. During the “absolute refractory period” no spikes can be generated. During the “relative refractory period” spikes can be generated but a larger applied current is needed. The absolute period follows immediately after a spike and the relative refractory period comes after the absolute period.

This phenomenon has important ramifications for hearing. For example, it indicates that the AN delivers auditory stimuli to the brain as a sequence of discrete inputs. In designing a cochlear implant, an understanding of the refractory effect is important because the refractory effect gives an upper bound for the frequency of electrical pulses that the auditory system can properly process. In particular, a cochlear implant that delivered pulses within the absolute refractory period or pulses during the relative refractory period that were not strengthened to account for the refractory effect, would not improve the hearing of the patient.

Figures 4 and 5 provide evidence that the FH model can capture the refractory effect.

In Figure 4, a 1mA pulse was delivered for 0.1msec at $t = 0$ msec (top plot). Then a second pulse of the same current was delivered at $t = 1$ msec (middle plot) and $t = 2$ msec (bottom plot). The plots show that the second pulse generates a spike after 2msec, but not after 1msec. This indicates that at $t = 1$ msec, the neuron is within the refractory period.

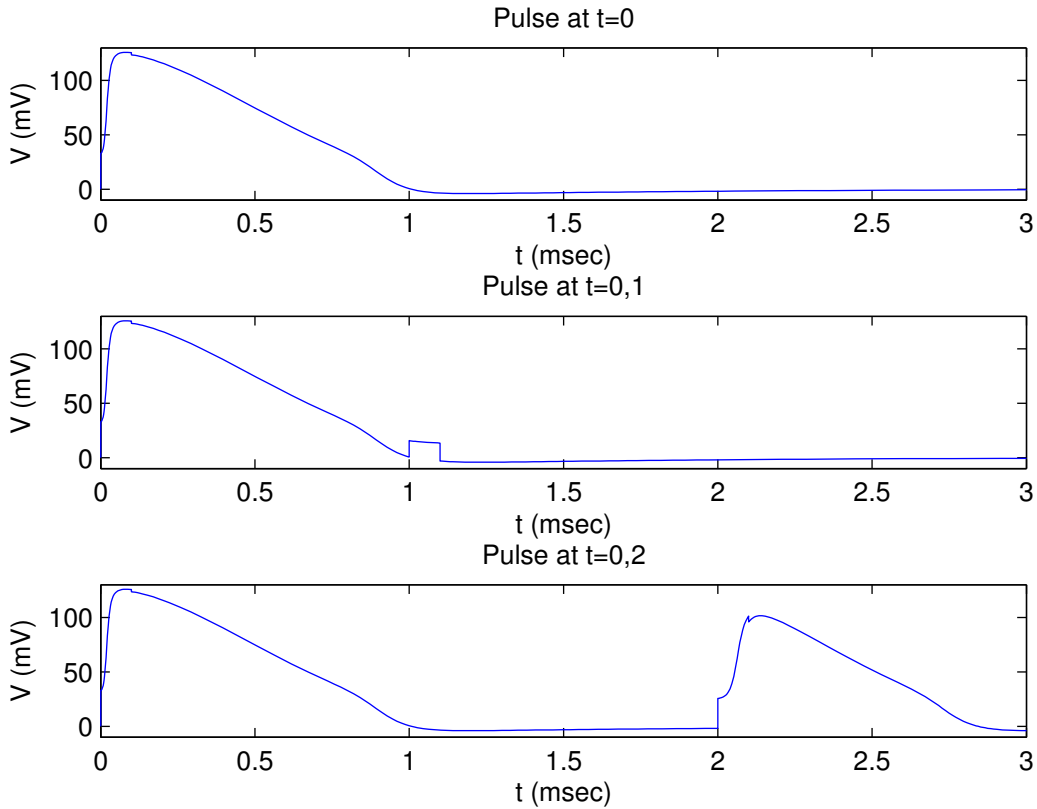


Figure 4: Modeling the Refractory Effect

Figure 5 displays the characteristics of the relative refractory period.

To create Figure 5, a 1mA pulse was delivered for 0.1msec at $t = 0$ msec (top plot), and then a second pulse of duration 0.1msec was delivered at $t = 1.5$ msec. In the middle plot, the second pulse is 1mA and no spike is generated. In the bottom plot, the strength of the pulse is increased to 2mA and a spike is generated in this case.

The refractory effect can be analyzed mathematically in terms of the stability of equilibrium points. As discussed previously, generation of a spike is modeled by perturbation away from an unstable equilibrium. If no such unstable equilibrium exists then generation of a spike would not be possible. Following Borisyuk and Rinzel (2004), we again make the simplifying assumptions of fast and slow variables and consider the instantaneous current as a function of voltage to investigate the existence and stability

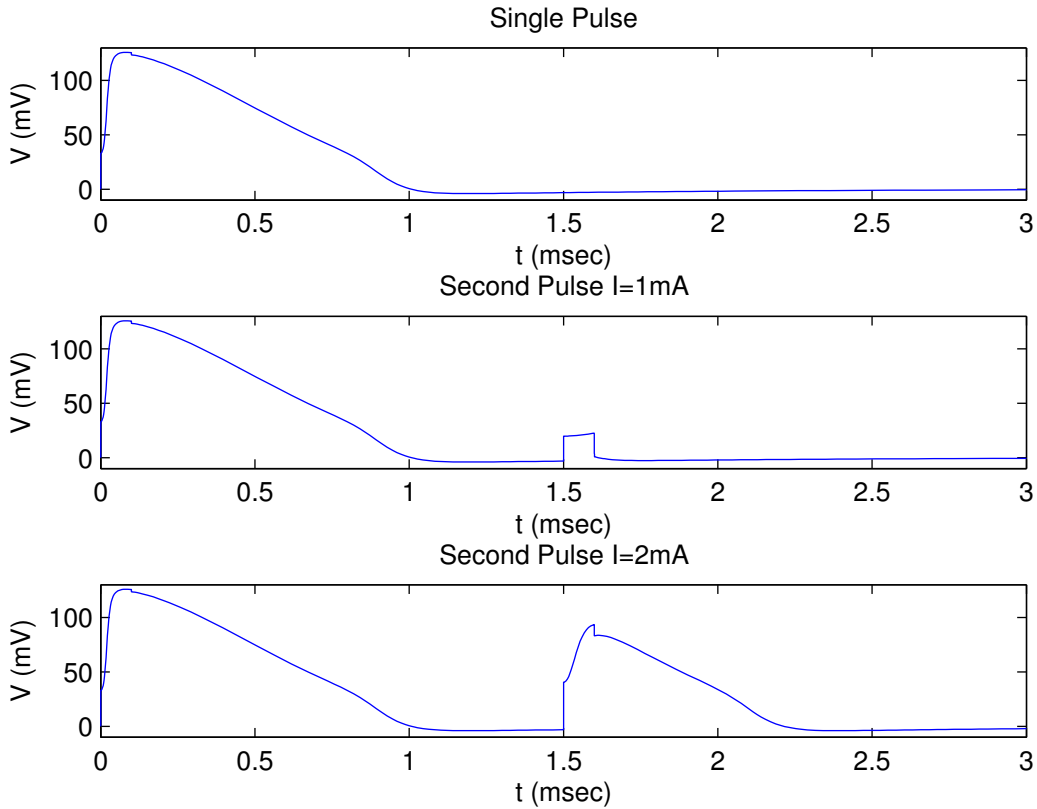


Figure 5: Modeling the Relative Refractory Period

of the equilibria of the system. We consider the case of a single pulse (1mA, duration 0.1msec), and explore how I_{inst} changes at different times throughout the generation of a spike and the return to the steady state.

Since our assumptions are valid only on short timescales, the voltage curve (Figure 1) is divided into four distinct periods. Borisyuk and Rinzel label these periods as the upstroke (generation of action potential), the plateau (very high voltage state), the downstroke (return to normal voltage levels), and the recovery (return to equilibrium state). In Table 1, the approximate identification of these phases is reported with respect to the simulation pictured in Figure 1.

Phase	Begin Time	End Time
Upstroke	0.0	0.1
Plateau	0.1	0.6
Downstroke	0.6	1.0
Recovery	1.0	3.0

Table 1: Phases of Voltage in Figure 1

Figure 6 shows the shape of the instantaneous current curve at the four different stages.

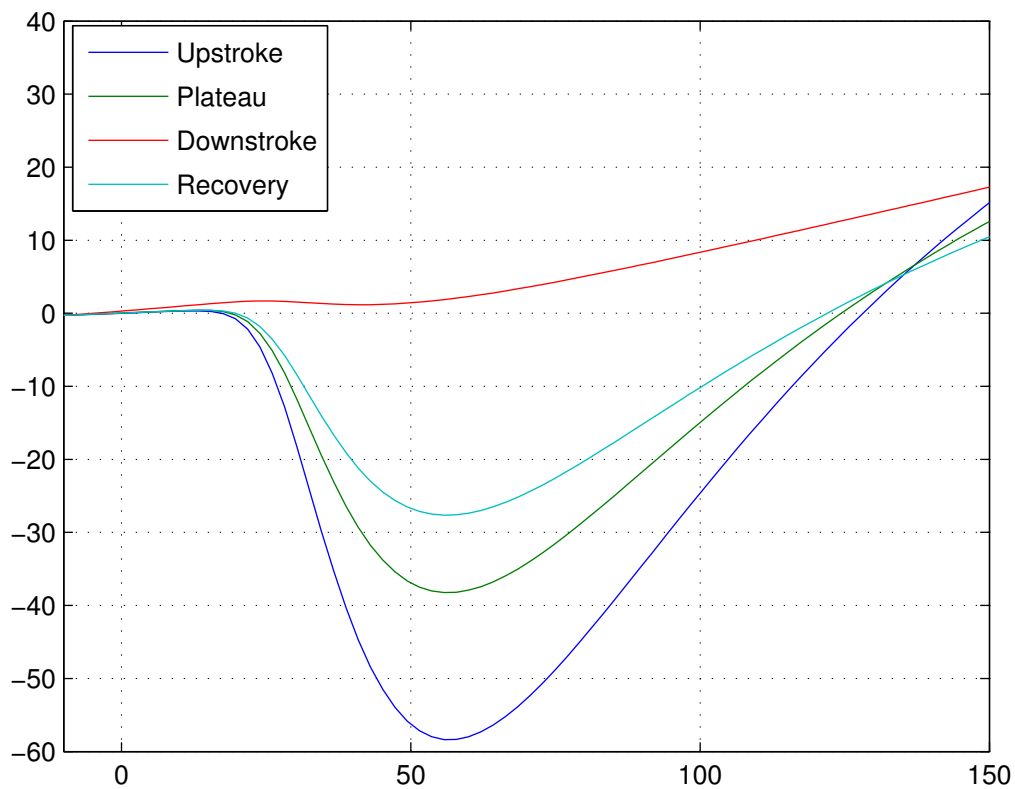


Figure 6: Changes in the Instantaneous Current over time

Of particular interest is the transition into and out of the downstroke phase. It is characterized by the fact that I_{inst} has only a single root. This corresponds to the

system having only a single equilibrium point during this phase. Since the slope of I_{inst} is positive here, the equilibrium point is stable. Interpreting this result in terms of the refractory effect, we see that the FH model predicts an absolute refractory period. Even if a current is applied during this period no spikes will be generated because the system will quickly settle back down to the unique (stable) equilibrium point.

In terms of the system of differential equations, we can say that a bifurcation occurs in between the plateau and downstroke when the system changes from having three equilibria to having a single equilibrium point. A second bifurcation occurs in the transition from the downstroke to the recovery when the two equilibria points reappear. These bifurcation points model the beginning and end of the absolute refractory period.

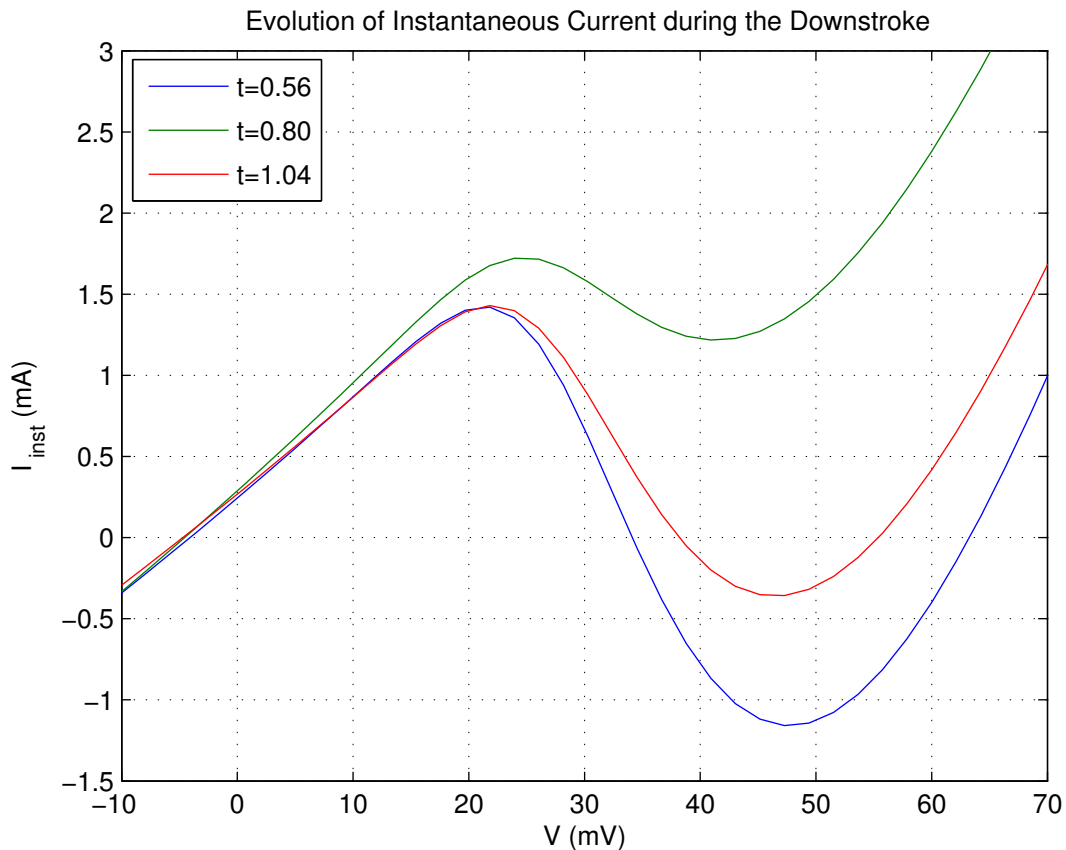


Figure 7: Bifurcation: The number of equilibrium points changes with time from three before the downstroke (0.56msec) to one during the downstroke (0.80msec) and back to three after the donwstroke. (1.04msec).

Figure 7 displays the dynamic of the bifurcation. Initially the curve has three roots representing three equilibria in the system. After the upstroke, the I_{inst} curve shifts upward during the plateau phase until it only intersects the V-axis once. During the downstroke it only has a single root corresponding to a single equilibrium point of the system. Then during the recovery phase it shifts back down and regains the two roots that it had lost in the immediate aftermath of the spike generation.

5 Conclusion

The auditory system converts acoustic stimuli into electrical pulses applied to the auditory nerve. The AN then relays this electrical pulse to the brain through the mechanism of action potentials. Studying the generation of action potentials and the AN response to electrical pulses is critical, therefore, to a more complete understanding of the auditory process. Additionally, this knowledge can be useful in developing cochlear implants to treat individuals with hearing disorders.

In this paper we have modeled the response of the AN to electrical pulses using a deterministic model of the Hodgkin-Huxley type. While there are limitations to modeling the AN as a deterministic process, our simplified model has proven to be mathematically tractable and it has displayed two important features of neural dynamics: the generation of action potentials and the existence of a refractory effect. Both of these observed physiological phenomena can be represented and analyzed mathematically in terms of the existence and stability of equilibrium points and bifurcations in the number of equilibria. The results have been obtained through numerically solving the Frankenhauser-Huxley system of ordinary differential equations with MATLAB and by analysing a version of the model that has been simplified by making assumption about the relative speed of the dynamics of the dependent variables in the equations.

Since the auditory nerve has a physiology distinct from other types of nerve cells,

future work should try to more closely model these characteristics. In particular, the McNeal model used by Colombo and Parkins, and the stochastic elements of Bruce et al should be investigated.

6 MATLAB Code

6.1 FH Model Equations

```
% This is frankhux.m
% It defines the differential equations that make up
% the Frankenhauser-Huxley Model
function dy = frankhux(t,y);
    dy = zeros(5,1);
    m = y(1);
    n = y(2);
    h = y(3);
    p = y(4);
    V = y(5);
[alphan,alphan,alphah,alphap,betam,betan,betah,betap,Ii] =parameter(m,n,h,p,V,t);
Cm=2*10^-6;
if (t>0 & t<.1) % Initial Pulse
    Ia=1; % Pulse Strength
%elseif (t>2.0 & t<2.1) % Subsequent pulses
%    Ia=1; % Pulse Strength
else Ia=0;
end;
%dm/dt
dy(1) = alphan*(1-m) - betam*m;
%dn/dt
dy(2) = alphan*(1-n) - betan*n;
%dh/dt
dy(3) = alphah*(1-h) - betah*h;
%dp/dt
dy(4) = alphap*(1-p) - betap*p;
% dV/dt
dy(5) = (1/Cm) * (Ia-Ii);
```

6.2 Parameters

```
% This is parameter
% It defines input parameters for the FH Model used in FH and CP
function [alphan,alphan,alphah,alphap,betam,betan,betah,betap,Ii] ...
    = parameter(m,n,h,p,V,t);
```

% Parameter Values (see FH paper)

```
Cm = 2*10^-6;
gl = .0303; % per ohm
Vl = 0.026;
PPna = 8*10^-3;
PPk = 1.2*10^-3;
PPp = 0.54*10^-3;
Er = -70;
F = 96.514; % per millimole
R = 9.3144;
T = 310.65;
Nao = 114.5*10^0;
Nai = 13.74*10^0;
Ko = 2.5*10^0;
Ki = 120*10^0;
Aam = 0.36;
Aan = 0.02;
Aah = 0.1;
Aap = 0.006;
Abm = 0.4;
Abn = 0.05;
Abh = 4.5;
Abp = 0.09;
Bam = 22;
Ban = 35;
Bah = -10;
Bap = 40;
Bbm = 13;
Bbn = 10;
Bbh = 45;
Bbp = -25;
Cam = 3;
Can = 10;
Cah = 6;
Cap = 10;
Cbm = 20;
Cbn = 10;
Cbh = 10;
Cbp = 20;
E = V+Er;
Pna = PPna * h * m^2;
Pk = PPk * n^2;
Pp = PPp * p^2;
Ina = Pna * ((E*F^2)/(R*T)) * ((Nao-Nai*exp((E*F)/(R*T)))/(1-exp((E*F)/(R*T))));
```

```

Ik = Pk * ((E*F^2)/(R*T)) * ((Ko -Ki*exp((E*F)/(R*T)))/(1-exp((E*F)/(R*T))));
Ip = Pp * ((E*F^2)/(R*T)) * ((Nao-Nai*exp((E*F)/(R*T)))/(1-exp((E*F)/(R*T))));
Il = gl * (V-Vl);
Ii = Ina + Ik + Ip + Il;
alphah = Aah*(Bah-V) / (1-exp((V-Bah)/Cah));
alphan = Aam*(V-Bam) / (1-exp((Bam-V)/Cam));
alphan = Aan*(V-Ban) / (1-exp((Ban-V)/Can));
alphap = Aap*(V-Bap) / (1-exp((Bap-V)/Cap));
betah = Abh / (1+exp((Bbh-V)/Cbh));
betam = Abm*(Bbm-V) / (1-exp((V-Bbm)/Cbm));
betan = Abn*(Bbn-V) / (1-exp((V-Bbn)/Cbn));
betap = Abp*(Bbp-V) / (1-exp((V-Bbp)/Cbp));

```

6.3 Bifurcation Analysis

```

% Bifurcation Analysis during refractory period
% Define the Instantaneous Current curve
% whose roots and slope determine the number and
% stability of Equilibrium points on a short timescale
j=[1:192];
sizej= size(j);
VV = linspace(-10,200);
for i=1:sizej(2)
%Slow timescale variables
h0 = h(j(i));
p0 = p(j(i));
n0 = n(j(i));
%Fast timescale variable m
alphaminf = Aam*(VV-Bam) ./ (1-exp((Bam-VV)./Cam));
betaminf = Abm*(Bbm-VV) ./ (1-exp((VV-Bbm)./Cbm));
minf = alphaminf./(betaminf+alphaminf);
% Compute parameters
Einst = VV+Er;
Pnainst = PPna * h0 * minf.^2;
Pkinst = PPk * n0^2;
Ppinst = Ppp * p0^2;
Inainf = Pnainst .* ((Einst*F^2)/(R*T)) .* ...
        ((Nao-Nai*exp((Einst*F)/(R*T)))/ ...
        (1-exp((Einst*F)/(R*T))));
Ik0 = Pkinst * ((Einst*F^2)/(R*T)) .* ...
      ((Ko -Ki*exp((Einst*F)/(R*T)))/ ...
      (1-exp((Einst*F)/(R*T))));
Ip0 = Ppinst * ((Einst*F^2)/(R*T)) .* ...
      ((Nao-Nai*exp((Einst*F)/(R*T)))/ ...

```

```

        (1-exp((Einst*F)/(R*T)))));
I10 = g1 * (VV-V1);
% Compute Instantaneous Current: Iinst(V,n0,h0,p0,minf)
Iinst = Inainf+Ik0+Ip0+I10;
IInst(:,i) = Iinst;
end;
plot(VV,IInst)

```

7 References

- A. Borisyuk (2005). Physiology and mathematical modeling of the auditory system. In: *Tutorials in Mathematical Biosciences I. Mathematical Neurosciences, Lecture Notes in Mathematics*, Vol. 1860, Springer, Berlin Heidelberg New York, 2005.
- A. Borisyuk and J. Rinzel (2004). Understanding neuronal dynamics by geometrical dissection of minimal models. In: *Methods and Models in Neurophysics, Les Houches Summer School, Session LXXX*, C. Chow, B. Gutkin, D. Hansel and C. Meunier (eds). Elsevier, 2004.
- I.C. Bruce, M. White, L. Irlicht, S. O’Leary, S. Dynes, E. Javel, and G. Clark (1999a). A stochastic model of the electrically stimulated auditory nerve: single-pulse response. *IEEE Trans. Biomed. Eng.* 46(6):617-629.
- I.C. Bruce, L. Irlicht, M. White, S. O’Leary, S. Dynes, E. Javel, and G. Clark (1999b). A stochastic model of the electrically stimulated auditory nerve: pulse-train response. *IEEE Trans. Biomed. Eng.* 46(6):630-637.
- J. Colombo and C.W. Parkins (1987). A model of electrical excitation of the mammalian auditory-nerve neuron. *Hear Res.* 31(3):287-311.
- R. Fitzhugh (1960). Thresholds and plateaus in the Hodgkin-Huxley nerve equations. *J. Gen Physiol.* 43:867-896.
- B. Frankenhauser and A.F. Huxley (1964). The action potential in the myelinated fiber of *Xenopus laevis* as computed on the basis of voltage clamp data. *J. Physiol.* 171:302-315.
- C. D. Geisler (1998). *From Sound to Synapse*. Oxford University Press, Oxford, 1998.
- J.D. Murray (2002). *Mathematical Biology, Vol. 1: An Introduction*. Springer, New York, 2002.